aerospace

MDPI

Article

Numerical Investigation of the Effect of Equivalent Ratio on Detonation Characteristics and Performance of CH_4/O_2 Rotating Detonation Rocket Engine

Xiao Xu [1], Qixiang Han [1,*] and Yining Zhang [2]

[1] College of Energy and Power Engineering, Nanjing University of Aeronautics and Astronautics, Nanjing 210016, China; bz2202002@nuaa.edu.cn
[2] Beijing Power Machinery Institute, Beijing 100074, China; zhangyining@casic.com.cn
* Correspondence: hqx205@nuaa.edu.cn

Abstract: Equivalent ratio (ER) is an important factor affecting detonation characteristics and propulsion performance of rotating detonation rocket engine (RDRE). In this paper, the effects of different equivalent ratios detonation characteristics and thrust performance of methane-oxygen RDRE were studied by 2D numerical simulation. The premixed reactants were injected through the injection holes to simulate the discrete injection of reactants on the injection panel in actual RDRE, the number of injection holes was 60 and 120. The results show that there is hybrid detonation mode (HDM), co-direction multi-wave detonation mode (CMM) and unstable detonation mode (UDM) in detonation combustion due to the influence of equivalent ratio and the number of injection holes, and the co-directional multi-wave detonation mode is beneficial to the thrust stability of RDRE. At the last, the number of detonation waves in RDRE decreases with the increase in the equivalent ratio, and the specific impulse (I_{sp}) increases with the increase of the equivalent ratio.

Keywords: equivalent ratio; detonation characteristics; propulsion performance

Academic Editors: Pedro Miguel Rebelo Resende, Mohsen Ayoobi and Alexandre M. Afonso

Received: 3 December 2024
Revised: 13 January 2025
Accepted: 14 January 2025
Published: 18 January 2025

Citation: Xu, X.; Han, Q.; Zhang, Y. Numerical Investigation of the Effect of Equivalent Ratio on Detonation Characteristics and Performance of CH_4/O_2 Rotating Detonation Rocket Engine. *Aerospace* **2025**, *12*, 68. https://doi.org/10.3390/aerospace12010068

1. Introduction

Detonation is a combustion process characterized by the strong coupling of shock waves and chemical reactions. As the detonation wave propagates through the reactants, its high temperature and pressure cause spontaneous ignition. Theoretically, detonation offers an exceptionally efficient method for combustion [1]. It has the advantages of high thermal cycle efficiency and fast heat release speed [2–6]. Compared to deflagration, detonation can achieve more intense and thermodynamically favorable fuel combustion within a smaller combustion chamber [7]. Therefore, the utilization of detonation as a novel approach to enhance the performance of ramjet and rocket engines has garnered significant attention [5], leading to the development of numerous prototypes for rotating detonation engines (RDEs) and rotating detonation rocket engines (RDREs).

The RDE combustion chamber typically adopts a ring structure, with fresh reactants being sprayed from the head of the chamber. After ignition, the rotating detonation wave (RDW) propagates around the combustion chamber. The detonation product is ejected at high speed from the bottom of the combustion chamber to produce continuous and stable thrust. However, due to the instability of RDE [8,9] and propellant equivalent ratio (ER), many problems still need to be studied.

In experimental investigations, Bykovskii et al. [10] validated the rotating detonation wave in liquid rocket and ramjet engines using air and liquid oxygen as oxidants, and

ascertained the control parameters for attaining continuous rotating detonation. Fotia et al. [11] carried out experimental studies on the performance of RDEs with nozzles and measured the equivalence ratio to explore the relationship between specific impulse and thrust. Russo et al. [12] analyzed the pressure rise characteristics of RDW and discovered that the propagation speed of RDW declines as the equivalence ratio decreases. Anand et al. [13] studied the propagation characteristics of hydrogen/air RDE under different injection modes, and the results showed that the ratio of reactant filling height to cell width of detonation gradually decreased under lean-fuel and rich-fuel conditions, and the rise of static pressure generated in RDE depends on the equivalent ratio of flow rate and reactant. Li et al. [14] studied the RDW propagation characteristics of hydrogen/air mixtures under various equivalence ratios and found that the average propagation frequency and speed of the RDW initially increase and subsequently decrease as the equivalence ratio rises. Deng et al. [15] found that RDE has the ability to adapt to the change in the equivalent ratio. The decrease of equivalent ratio leads to the deterioration of the reactivity of the mixture, which reduces the wave velocity in single-wave mode and leads to the conversion of the two-wave mode to single-wave mode. Xie et al. [16] examined the combustion modes of the H2/Air RDE with air mass flow rates ranging from 25 to 225 g/s and equivalence ratios from 0.6 to 1.0, identified four combustion mode subregions, including fast deflagration, unstable detonation, quasi-stable detonation, and stable detonation.

In numerical simulations, Wang et al. [17] conducted numerical studies on three-dimensional Hydrogen/Air RDE and found that the RDW propagation speed initially increases and then decreases as the equivalence ratio increases. In 2020, Zheng et al. [18] conducted numerical studies on hydrogen/air non-premixed RDE under different equivalent ratios, and the results showed that with the increase of equivalent ratio, the mode of RDW changed from single wave mode to double wave mode, and the change of equivalent ratio had an impact on the specific impulse and thrust of RDE. Zhao et al. [19,20] conducted a two-dimensional numerical study on the RDE of hydrogen/air premixed mixtures. It was found that the detonation wave number and propagation direction change with the increase in injection pressure, and the equivalent ratio is also one of the factors causing RDW chaotic propagation. Lietz et al. [21] used the large eddy simulation method to study the effects of equivalent ratio and mass flow rate on combustion performance of methane-oxygen RDRE. The results showed that increasing mass flow rate would increase combustion chamber pressure, thrust, and specific impulse, while increasing equivalent ratio would cause detonation waves change into bidirectional or flatting mode, which could not produce significant performance gain. Huang et al. [22,23] studied the expansion characteristics of nozzle and the effect of equivalent ratio on the thrust of RDE, and the results showed that the addition of a nozzle could improve RDE thrust, and the specific impulse of RDE increased with the increase of equivalent ratio. Yao et al. [24] studied the spontaneous formation of multiple detonation wavefronts in RDE through three-dimensional numerical simulation, and the results showed that the explosion caused by the collision of detonation wavefronts could induce new detonation waves and possibly change the propagation direction. The numerical study of Wu et al. [25] shows that the double wave mode improves the stability of RDE combustor, and the average outlet pressure in the double wave mode is higher than that in the single wave mode. Zhou et al. [26] found that oblique shock waves have little effect on RDE performance through two-dimensional numerical simulation, and the detonation thermodynamic cycle model in numerical simulation is consistent with the ideal ZND model. Subramanian et al. [27] found that detonation and deflagration existed simultaneously in RDE through two-dimensional numerical study, and stratification of fuel and product would cause the detonation wave velocity to decrease. Chen et al. [28] found that with the change of equivalent ratio, the propagation mode of RDW changes

from single wave to double wave in the same direction and double wave collision. The velocity deficit of RDW in double wave mode is larger than that in single wave mode, specific impulse decreases with the increase of equivalent ratio and specific thrust increases with the increase of equivalent ratio in single wave mode.

According to the above research, it was found that there are many factors affecting RDW propagation characteristics and propulsion performance, and the equivalent ratio is one of the important influencing factors. The chemical characteristics of reactants, reaction heat release rate, detonation wave velocity, and propagation stability are all affected by the equivalent ratio. Therefore, the effect of equivalent ratio on RDW propagation mode and propulsive performance has important research value. Two-dimensional numerical simulations of premixed CH_4/O_2 RDRE with 60 and 120 injection holes were carried out under different equivalent ratios to solve these problems. Different from the ramjet RDE, RDRE operates in the fuel-rich range and it is necessary to study the detonation combustion characteristics and propulsion performance of RDRE under different equivalent ratios and high inlet total pressure. The purpose of this paper is to investigate the influence of equivalent ratio on detonation combustion characteristics and RDW propagation modes of RDRE with varying numbers of holes, as well as to examine the impact of different RDW propagation modes on the propulsion performance of RDRE.

2. Numerical Methods and Computational Models

2.1. Numerical Method

Fluent is used for numerical simulation in this study, the simulation involves the high-speed flow process and chemical reaction process of fluid in rotating detonation, and the transport phenomena such as viscosity, thermal diffusion, and mass diffusion are considered. Therefore, two-dimensional compressible Navier-Stokes equations in cartesian coordinates are used in numerical simulation:

$$\frac{\partial U}{\partial t} + \frac{\partial F_1}{\partial x} + \frac{\partial F_2}{\partial y} = \frac{\partial G_1}{\partial x} + \frac{\partial G_2}{\partial y} + S \tag{1}$$

$$U = (\rho_1, \cdots, \rho_N, \rho u, \rho v, E)^T \tag{2}$$

$$F_1 = [\rho_1 u, \cdots, \rho_N u, \rho u^2 + p, \rho uv, u(E+p)]^T \tag{3}$$

$$F_2 = [\rho_1 v, \cdots, \rho_N v, \rho uv, \rho v^2 + p, v(E+p)]^T \tag{4}$$

$$G_1 = [\rho D_1 \frac{\partial Y_1}{\partial x}, \cdots, \rho D_N \frac{\partial Y_N}{\partial x}, \tau_{xx}, \tau_{xy}, q_x + u\tau_{xx} + v\tau_{xy}]^T \tag{5}$$

$$G_2 = [\rho D_1 \frac{\partial Y_1}{\partial y}, \cdots, \rho D_N \frac{\partial Y_N}{\partial y}, \tau_{yx}, \tau_{yy}, q_y + u\tau_{yx} + v\tau_{yy}]^T \tag{6}$$

$$S = [0, \cdots, 0, \rho f_x, \rho f_y, \rho(uf_x + vf_y) + \rho\dot{q}]^T \tag{7}$$

In the above equations, F_1 and F_2 are the convection vectors, G_1 and G_2 are the viscous convection fluxes, p, u, and v represent pressure, velocity in the x direction and velocity in the y direction, respectively, D is the Diffusion coefficient. The total energy E and the density ρ are calculated by:

$$\rho = \sum_{i=1}^{N} \rho_i, i = 1, 2, \cdots, N \tag{8}$$

$$E = \sum_{i=1}^{N} \rho_i h_i + \frac{1}{2}\rho(u^2 + v^2) \tag{9}$$

where h is the specific enthalpy.

The turbulence model adopted the SST k-ω model, which is detailed as follows, and the specific symbols and parameters should be seen in relevant literature [29]:

$$\frac{\partial}{\partial t}(\rho k) + \frac{\partial}{\partial x_i}(\rho k u_i) = \frac{\partial}{\partial x_j}(\Gamma_k \frac{\partial k}{\partial x_j}) + G_k - Y_k + S_k \tag{10}$$

$$\frac{\partial}{\partial t}(\rho \omega) + \frac{\partial}{\partial x_i}(\rho \omega u_i) = \frac{\partial}{\partial x_j}(\Gamma_\omega \frac{\partial \omega}{\partial x_j}) + G_\omega - Y_\omega + S_\omega \tag{11}$$

A coupled algorithm was used in this paper, the stiff chemical solver based on Arrhenius equation was used for the chemical reaction, and the FFCMy-12 [30] chemical mechanism was used to model the chemical reactions. This chemical mechanism has been successfully applied to the three-dimensional large eddy simulation (LES) numerical calculation of RDRE [21,31]. The second order upwind scheme was used for pressure discretization and the third order QUICK scheme was used for discretization of other spatial convection terms to achieve accurate solutions for the flow field. The second order implicit scheme was used for time discretization. The specific heat, thermal conductivity, and viscosity of the material are calculated by ideal gas mixture model based on kinetic theory.

2.2. Computational Model

The annular RDRE combustion chamber can be approximated as a two-dimensional computational domain for numerical analysis due to its small height relative to its diameter and limited radial variation imposed by the flow field, which helps save calculation resources. Although this approach neglects three-dimensional effects such as wall boundary layer, channel curvature, and detonation wave structure [32,33], numerous two-dimensional RDE numerical studies [23,34–41] have demonstrated that it effectively captures the key characteristics and flow field structure of rotating detonation propagation in RDRE, including the presence of detonation waves, oblique shock waves, contact surfaces between fresh reactants and combustion products, and slip lines.

The two-dimensional calculation model of RDRE is shown in Figure 1. The total length in x direction is 300 mm, the total height in y direction is 95 mm, the height of the plenum is 20 mm, the height of the injection holes is 5 mm, and the height of the combustion zone is 70 mm. Since the reactants in the experiment are usually injected into the combustion chamber through small holes or slits, discrete injection holes were used to simulate the discrete distribution of the reactants in practice in this paper. The injection hole of the calculation domain is shown in Figure 1. The inlet boundary is alternatively distributed by both the inlet and the wall. The wall is the adiabatic slip boundary. The total number of injection holes is 60 and 120, with a consistent injection area. The ratio between the injection holes and the wall is ¼ . The patch method is adopted for detonation ignition, the specific location is shown in Figure 1. The size of the ignition region is 10 mm × 10 mm square, the ignition temperature is 2000 K, and the pressure is 2 MPa. At the same time, the ignition region is given at a speed of 2000 m/s in the x direction. The red and dark blue regions are filled with the premix CH_4/O_2 gas from the plenum, which is maintained at the pressure of 1 MPa and at the temperature of 300 K. The equivalent ratio is set according to the requirements of different cases. The gas composition in the yellow region is modified from CH_4/O_2 premixed gas to CO_2/H_2O premixed gas with a mass ratio of 1:1 by patch method. A non-reflecting pressure outlet boundary is applied at the outlet, where the conditions are set to the ambient temperature (300 K) and pressure (101,325 Pa). It should be noted that chemical reactions in the regions of injection holes and plenum are shut off to prevent flame flash back into the plenum.

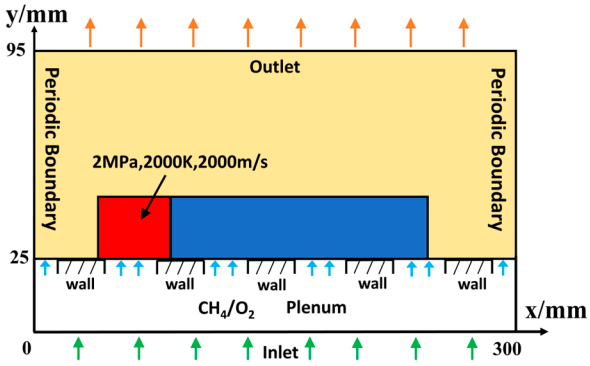

Figure 1. Two-dimensional RDRE calculation domain.

3. Verification of Numerical Simulation Method

A 40 cm long two-dimensional detonation tube is numerically simulated and compared with the Chapman-Jouguet (C-J) theoretical velocity and theoretical temperature calculated by NASA CEA [42] to verify the reliability of the numerical method and the mesh size. Three mesh sizes of 0.2 mm, 0.4 mm, and 0.5 mm were used to verify the mesh resolution. The detonation tube is filled with methane-oxygen premixed gas with an equivalent ratio of 1, a gas pressure of 101,325 Pa and a gas temperature of 300 K. Figure 2 depicts the distribution of detonation pressure with three different grid resolutions. The distribution of pressure drop in the three grids is basically the same, which means that the grid resolution has been reasonably converged. Therefore, a mesh size of 0.4 mm is used in numerical simulation to ensure the calculation accuracy and save the calculation resources. Figure 3 shows the distribution of detonation wave pressure and velocity at different times with 0.4 mm grid. In this study, the propagation velocity and the temperature of detonation wave are 2659 m/s and 3958 K, the C-J theoretical velocity is 2390 m/s with an error of 11% and the C-J theoretical temperature is 3721 K with an error of 6.4%. The results show that the simulation results are in good agreement with the C-J theoretical value calculated by NASA CEA. Due to the high activity of oxygen as an oxidizer, the simulation results are acceptable in this paper and the reliability of the numerical method in this study can be verified from C-J velocity and C-J temperature. The method proposed in this paper is suitable for the two-dimensional numerical study of methane-oxygen detonation in compressible reactive fluids.

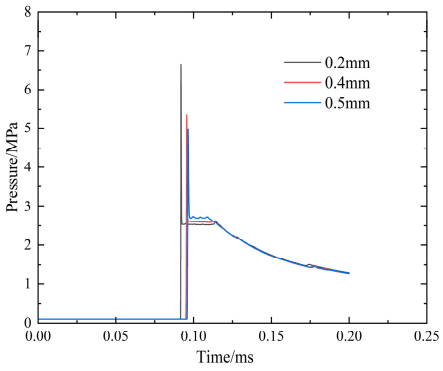

Figure 2. Pressure distribution of different grid numbers.

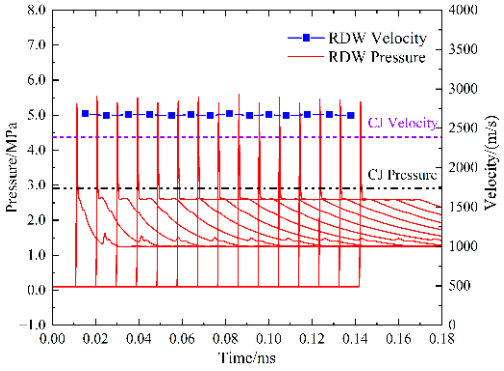

Figure 3. Pressure and velocity distribution in 0.4 mm grid at different times.

Figure 4 shows the comparison between the numerical simulation flow field in this study and the experimental results of Bykovskii et al. [10]. The numerical simulation of methane-oxygen RDRE with a total inlet temperature of 300 K, a total pressure of 1 MPa and an equivalent ratio of 1.4. The result shows that the numerical flow field structure in this study is consistent with the propane-oxygen RDE flow field structure obtained by Bykovskii et al. [10], which further verifies the reliability of the numerical calculation methods in this paper.

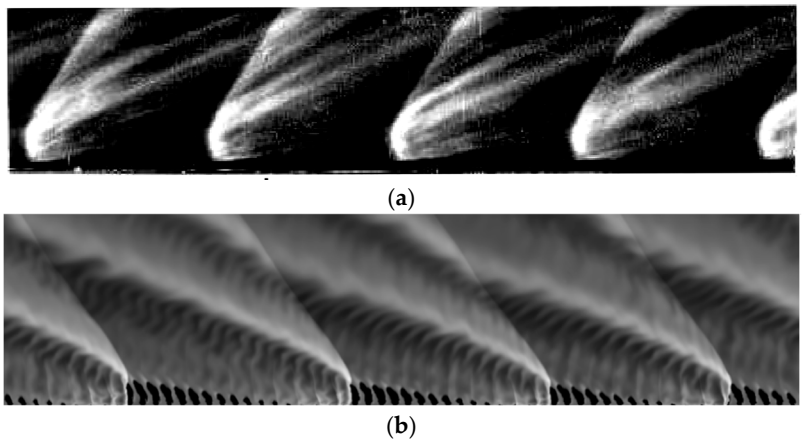

(**a**)

(**b**)

Figure 4. Comparison of numerical and experimental flow field. (**a**) Flow field structure of propane-oxygen RDE captured by Bykovskii et al. [10]. (**b**) Numerical flow field structure of RDRE in this study.

4. Results and Discussion

4.1. Influence of Equivalent Ratio on RDRE Flow Field Structure

This section discusses the effect of equivalent ratio on the structure of RDRE detonation flow field. RDRE simulation results under different equivalent ratios are shown in Table 1. P_{inlet} and T_{inlet} are the inlet total pressure and the inlet total temperature of premixed CH_4/O_2 in plenum. According to the results, there are three modes of detonation propagation. They are hybrid detonation mode (HDM), co-directional multi-wave mode (CMM), and unstable detonation mode (UDM). Detonation ignition failed in case B5, while the other cases are in detonation combustion mode.

Table 1. Numerical simulation results.

ER	P_{inlet}	T_{inlet}	60 Injection Holes			120 Injection Holes		
	MPa	K	Case	Wave Number	Mode	Case	Wave Number	Mode
1.0	1.0	300	A1	Unstable	HDM	B1	10	CMM
1.2	1.0	300	A2	6	CMM	B2	8	CMM
1.4	1.0	300	A3	4	CMM	B3	8	CMM
1.6	1.0	300	A4	3	CMM	B4	Unstable	UDM
1.8	1.0	300	A5	2	CMM	B5	Failure	Failure

When the number of injection holes is 60, two RDRE detonation flow field structures appear: the hybrid detonation mode with a large amount of deflagration in case A1 and the co-directional multi-wave mode in the other cases. As shown in Figure 5, the temperature and static pressure contours of RDRE flow field from top to bottom are case A1~A5. Since the flow field of the plenum and injection holes is not the focus of research, it is not discussed in this study.

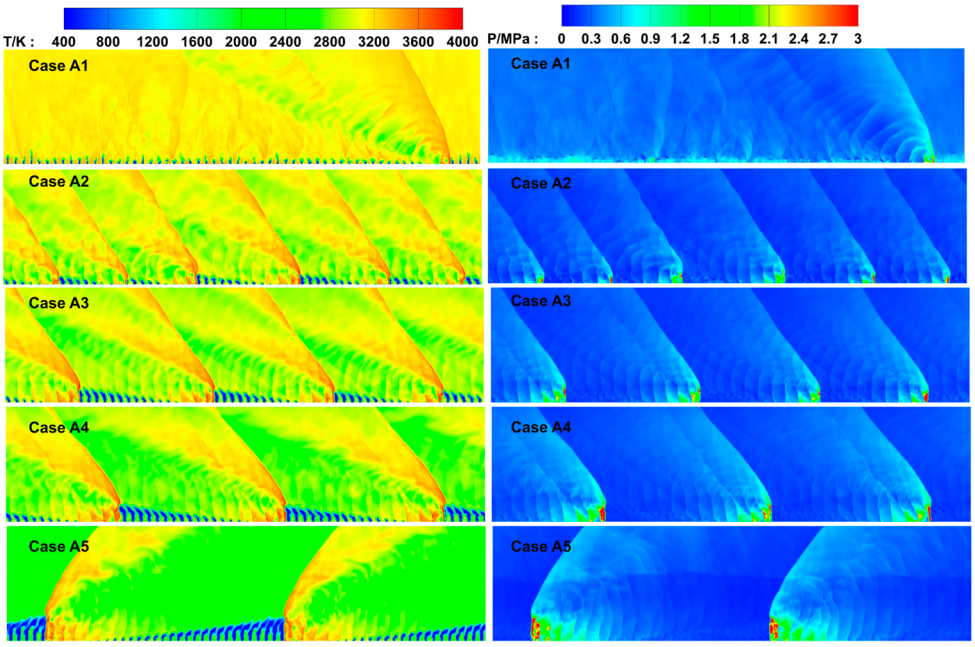

Figure 5. Contours of temperature and static pressure in case A1~A5.

As shown in Figure 6, the flow field of case A4 is a typical two-dimensional multi-wave detonation flow structure, where A is the detonation wave, B is the oblique shock wave, C is the slip line, D is the contact surface, and E is the triangular reactant filling zone. The detonation wave and oblique shock wave are uniformly distributed, which is a standard multi-wave stable propagation structure of the detonation in the same direction, it is also consistent with the flow field structure simulated by Huang et al. [23]. The reactants enter the RDRE through the injection holes. After the detonation wave passes through, deflagration regions are distributed in strips. Under this condition, the proportion of deflagration in the reactant filling zone is small, because the high equivalent ratio reduces reactant activity, resulting in less heat accumulation in the deflagration zone, and large-scale deflagration could not be formed.

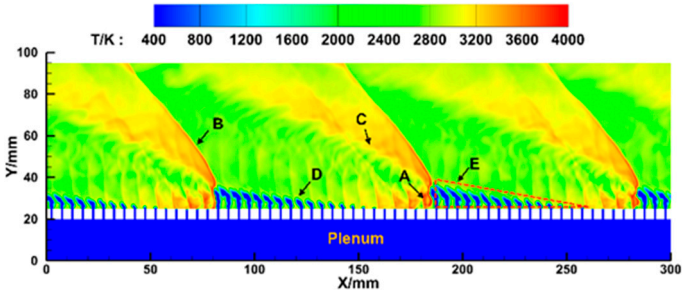

Figure 6. Contours of temperature in case A4.

The RDRE flow field structure of case A1 is relatively special. There are both detonation waves and a large amount of deflagration in the flow field, which belongs to the detonation-deflagration mixed combustion. The flow field structure of case A1 is similar to the tangential instability in conventional rocket engines. When ER = 1, the reactant activity is the highest, and the reactant starts to burn when it enters the combustion chamber, and a reactant layer of sufficient height cannot be formed. It also can be noted that the height of the reactant filling zone under this condition is the lowest. A large amount of fuel is consumed by deflagration, resulting in insufficient energy to support the propagation of detonation waves. Meanwhile, the accumulated heat of deflagration also induces the formation of new detonation waves. These two factors together lead to the instability of detonation wave propagation. Detonation-deflagration mixed combustion and any non-ideal, non-detonation processes are harmful to the performance of RDRE and will consume chemical energy and reduce the proportion of energy used by detonation [43,44]. The optimal combustion method in RDRE is to maximize the proportion of fuel used for detonation in the combustion chamber. Figure 7 shows the propagation process of detonation waves in case A1, and the number and direction of RDWs vary at different times.

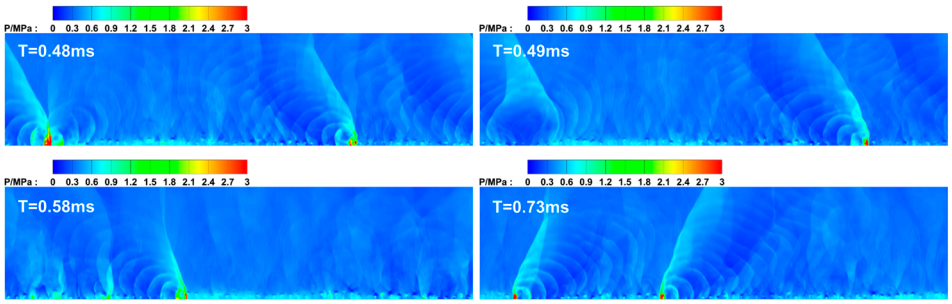

Figure 7. Contours of static pressure of case A1 at different time.

Figure 8 shows the local OH distribution contour of Case A1~A5. There is a qualitative positive correlation between the concentration of OH and the heat release rate, and the mass fraction of OH represents the magnitude of reaction intensity and heat release rate [45,46]. It can be clearly found that a large amount of deflagration occurs after fuel injection under condition A1. A large amount of OH was distributed around the injection holes and in the whole chamber. For the remaining cases, the OH mass fraction in the detonation wave front and post-wave regions decreases with the increase of the equivalent ratio, and the OH distribution is concentrated in the detonation wave and oblique shock wave regions, indicating that the decrease of deflagration ratio in RDRE and post-detonation wave region. The decrease in reactant activity leads to the decrease in heat release rate and intensity of detonation combustion, reduces the probability of inducing new detonation wave formation, reduces the number of detonation waves, and increases the proportion

of reactant used for detonation. In general, the decrease in reactant activity will lead to a decrease in the number of detonation waves in the RDRE and an increase in the height of the reactant filling zone, thus affecting the flow field structure in the RDRE.

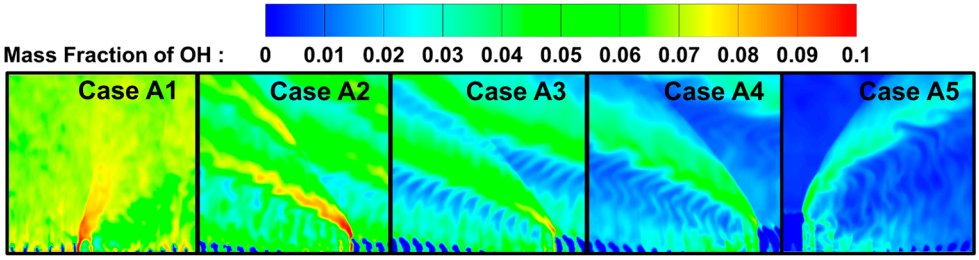

Figure 8. OH distribution contours of detonation wave front in case A1~A5.

When the number of injection holes is 120, CMM and UDM appear as shown in Figure 9. Figure 9 is the temperature and pressure contours of Cases B1~B4. The flow field structure in CMM will not be discussed. For UDM, take case B4 as an example, the flow field is in the state of unstable detonation propagation. As shown in Figure 10, in the unstable propagation mode, the number of detonation waves in the flow field is lower, the height of the reactant filling zone is higher, the distribution of detonation waves in the flow field is irregular, and linear oblique shock waves are not formed due to the impact of detonation wave collisions. When the detonation wave collides at t = 1.1 ms, the weaker detonation wave is decoupling and reburning after the collision, repeating the process of detonation wave collision, initiation, and annihilation, resulting in the unstable propagation mode of RDRE, Yao et al. [24] and Xia et al. [47] also observed a similar reinitiation phenomenon. The heat accumulated in small deflagration region is insufficient to induce the formation of RDW in the condition of low reactant activity, and even the deflagration in some areas disappears, such as the filling zone of the detonation wave front at t = 1.04 ms. The unsteady propagation mode eventually leads to the uneven distribution of temperature and pressure in the flow field and the uneven expansion of combustion products.

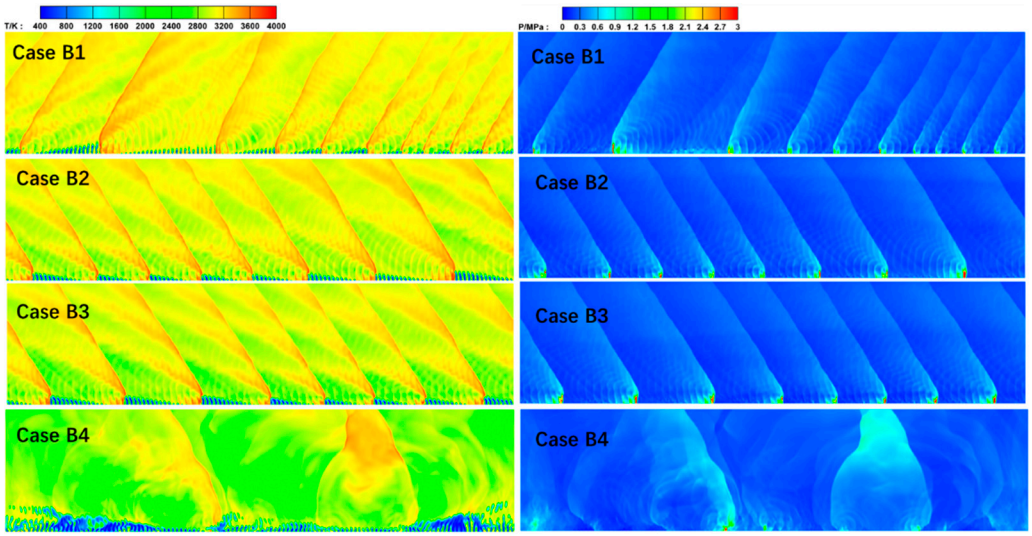

Figure 9. Contours of temperature and static pressure in cases B1~B4.

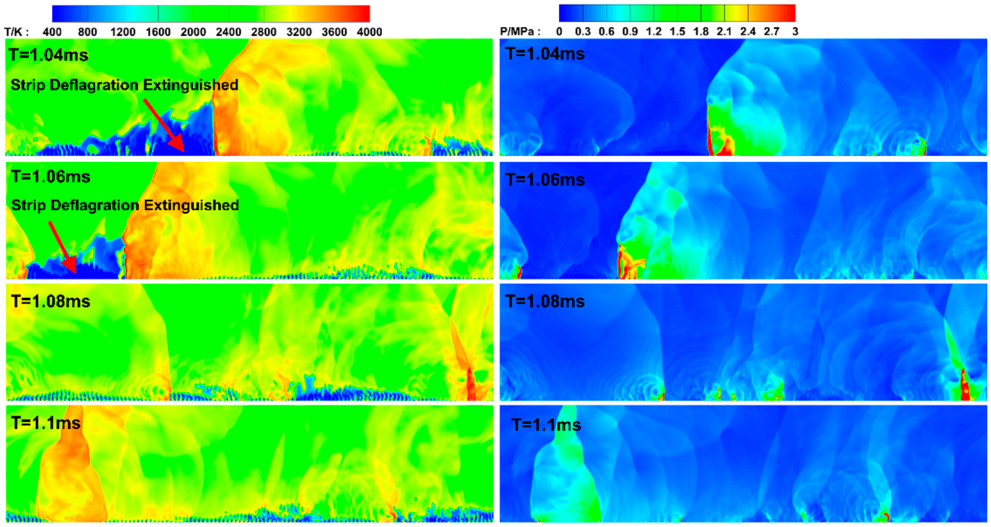

Figure 10. Detonation wave propagation process in case B4.

Different from case A1, case B1 does not operate in hybrid detonation mode. Figure 11 shows the contours of reaction heat in Case A1 and B1. It can be observed that a large amount of deflagration consumes reactants under the condition of high reactant activity, resulting in the accumulation of a large amount of reaction heat. It is known that hotspots easily form detonation wave under conditions of high reactant activity. However, excessive consumption of reactant during deflagration results in insufficient energy for the stable propagation of detonation waves [43,44], ultimately leading to unstable propagation.

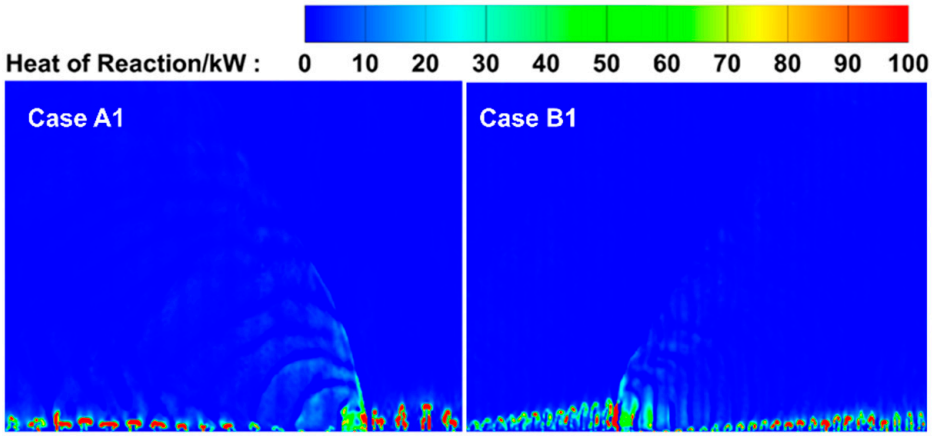

Figure 11. Heat of reaction counters in case A1 and case B1.

In conclusion, under the same inlet conditions, the increase in the number of injection holes improves the dispersion degree of the reactants, induces the formation of multi-wave propagation modes under the condition of high reactant activity (ER $\leq$ 1.4), and leads to the formation of more RDWs but reduces the accumulated heat in the deflagration region of the reactant filling zone. When the reactant activity is low (ER = 1.6) and the number of injection holes is 120, an unstable detonation propagation mode was formed, and the detonation failed at higher equivalent ratio. However, stable detonation is achieved with 60 injection holes under low reactant activity, because more heat accumulated in large strip deflagration regions increases the reactant activity. In general, the increase in the equivalent ratio leads to the decrease in reactant activity, resulting in a decrease of the probability of multiple detonation wave formation in the initiation stage, a decrease in the number of

RDWs and a decrease of the ratio of deflagration in RDRE. These also lead to an increase in the height of the reactant filling zone and RDWs. For optimal performance of RDRE, the ratio of detonation combustion should be maximized, and the detonation propagation mode should be in CMM.

4.2. Effect of Equivalent Ratio on Propagation Characteristics of RDW

The above research indicates that the equivalent ratio has a significant influence on the flow field of RDRE, thereby exerting a substantial impact on the propagation characteristics of RDW. Figures 12–14 illustrate the temporal evolution of static pressure and temperature at the sampling point of the RDRE (x = 90 mm, y = 28 mm). Figure 12 shows the temperature and static pressure history diagram of case A1. The static pressure and temperature curve shows that the propagation mode of condition A1 is in the single wave/multi-wave conversion mode. The arrows in the figure indicate the multi-wave region, where the single wave/multi-wave conversion is continuously carried out in the flow field. The reason for this chaotic pattern [48] is that hotspots around the reactants will lead to the formation of new detonation waves, while there are not enough reactants to maintain the intensity and propagation of the detonation waves, resulting in constant decoupling and re-initiation of the detonation waves. In addition, discrete injection holes will generate multiple reflected waves after the detonation wave, and stronger reflected waves may also be transformed into detonation waves [35,49]. According to previous studies, when the equivalent ratio is 1, the reactant activity is the largest, and a large number of hotspots near the injection holes can induce the formation of new detonation waves, but there are not enough reactants to maintain the stable propagation of detonation waves, and it is impossible to convert from chaotic mode to stable detonation propagation mode. Therefore, the HDM is an unstable propagation mode. Under the condition of 60 injection holes, a stable multi-wave propagation mode is formed. Except for case A1, the number of detonation waves in other stable propagation conditions shows a downward trend, and the time required to form a stable detonation mode is relatively similar. Meanwhile, the peak temperature and pressure of detonation wave are less affected by the changes in equivalent ratio. The peak temperature of detonation wave is around 3900 K, and the peak static pressure of the RDW is around 2 MPa.

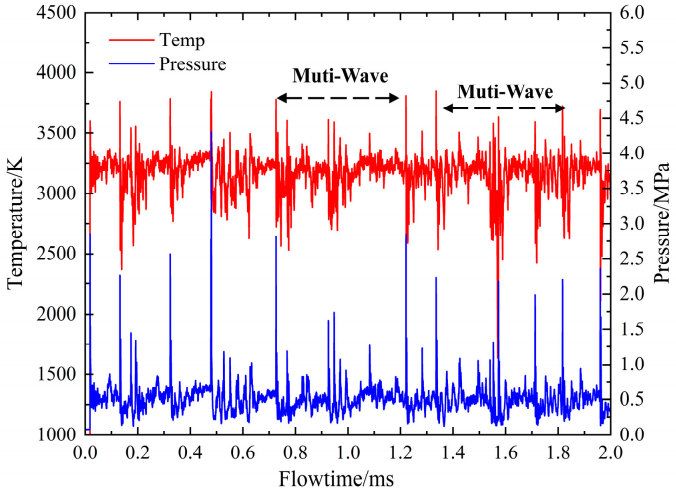

Figure 12. Pressure and temperature history diagram of case A1.

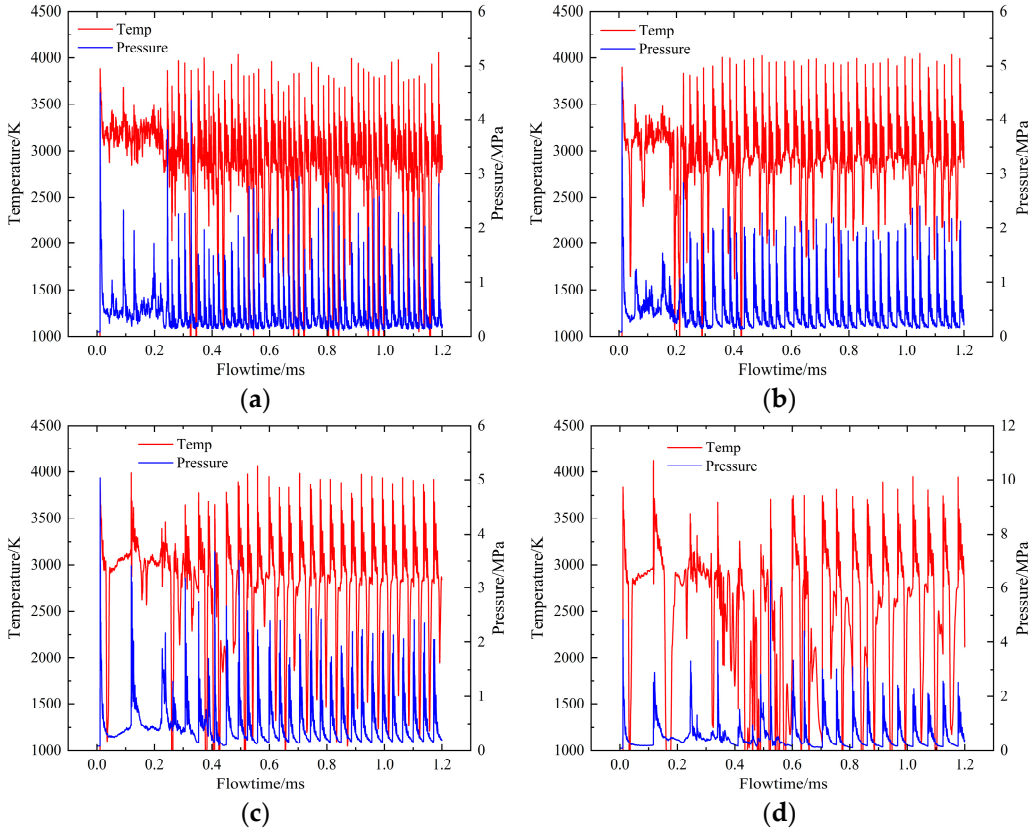

Figure 13. Pressure and temperature history diagram of case A2~A5. (**a**) Case A2. (**b**) Case A3. (**c**) Case A4. (**d**) Case A5.

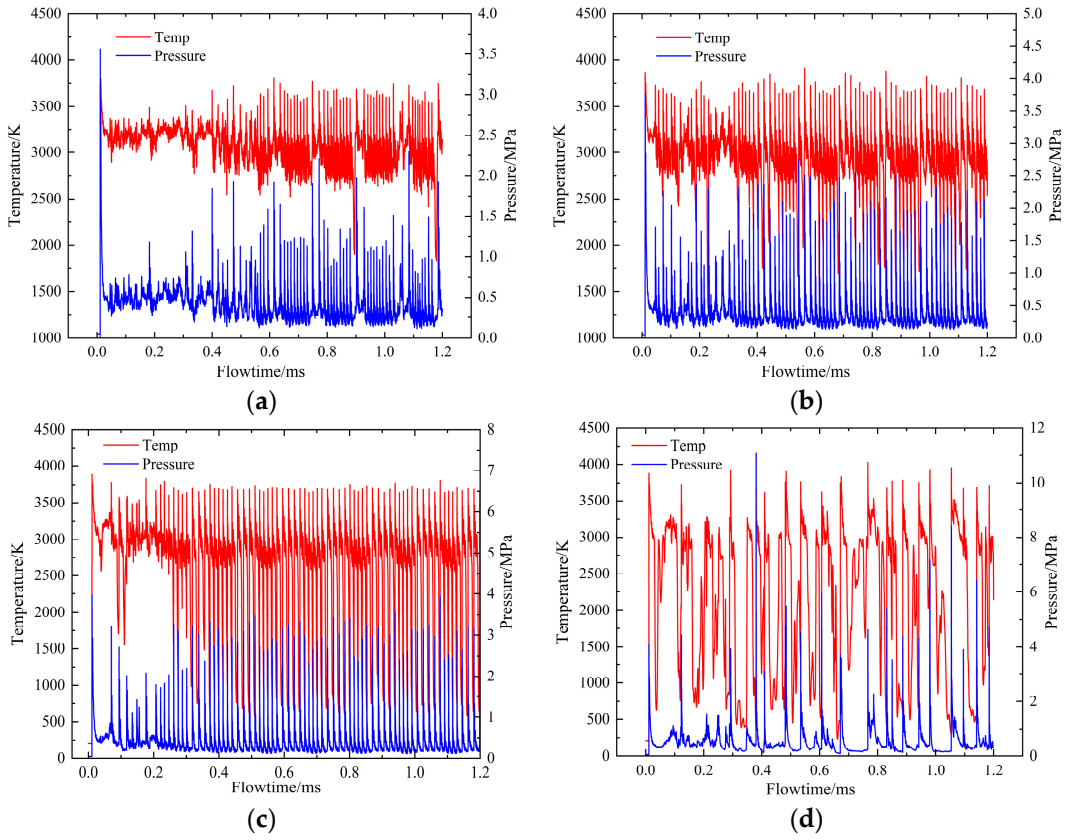

Figure 14. Pressure and temperature history diagram of cases B1~B4. (**a**) Case B1. (**b**) Case B2. (**c**) Case B3. (**d**) Case B4.

Figure 14 shows the static pressure and temperature history diagram of case B1, B2, B3, and B4 when the number of injection holes is 120. RDRE is in a stable multi-wave detonation propagation mode with equivalent ratios of 1, 1.2, and 1.4, the temperature and pressure peaks are coupled, and the flow field of RDRE is in a stable multi-wave propagation state. In case B1, with an equivalent ratio of 1, the peak temperature and pressure of RDW are significantly lower than those in other cases. This is primarily attributed to a higher proportion of reactants being consumed through deflagration rather than detonation, resulting in a lower intensity and pressure of RDW. The quantity of reactants consumed by deflagration in case B1, however, is insufficient to generate a detonation-deflagration mixing mode. When the equivalent ratio is 1.6, RDRE is in the UDM state, and it can be clearly observed that the peak pressure and temperature do not coincide, exhibiting an irregular distribution. It indicates that the detonation wave in the flow field is constantly colliding, annihilating, and reigniting. In general, as the equivalent ratio increases, there is a decreasing trend in the number of detonation waves with a closer formation time for stable detonation conditions. Simultaneously, changes in the equivalent ratio have less impact on the temperature and pressure of the detonation wave, the peak temperature of RDWs in cases B1~B3 reaches approximately 3700 K, the peak temperature is marginally lower compared to other cases with 60 injection holes under the same equivalent ratio and propagation mode. Meanwhile, the peak pressure of cases B2~B3 reaches around 2 MPa and the peak pressure of RDWs in case B1 is marginally lower compared to other cases due to a relatively reduced proportion of reactants used for detonation.

Table 2 shows the propagation velocity V_{DW} of RDWs at t = 1.2 ms and Δt_1 is the time for forming a stable co-directional multi-wave propagation mode under different equivalent ratios. The results show that with the increase of equivalent ratio, the propagation speed of RDW in stable propagation mode increases, and Δt_1 required to form stable co-directional propagation mode is within 1 ms. At the same equivalent ratio, the detonation wave propagation velocity of RDRE with fewer injection holes is faster, because more injection streams and strip deflagration regions hinder the propagation of detonation wave and resulting in the loss of detonation wave propagation velocity. On the other hand, the decrease in detonation wave velocity will also lead to the increase in the height of the filling zone, but the main factor affecting the height of the reactant filling zone is the number of detonation waves. Considering the different number of injection holes and fuel-rich conditions, stable co-directional multi-wave detonation propagation modes are more easily formed under equivalent ratio 1.2 and 1.4. However, when equivalent ratio is 1, due to the highest reactant activity, the increase in the deflagration fuel consumption ratio can form an HDM, which is not conducive to the detonation combustion of RDRE.

Table 2. V_{DW} and Δt_1 under different equivalent ratios.

ER	P_{inlet}	T_{inlet}	60 Injection Holes			120 Injection Holes		
	MPa	K	Case	Δt_1/ms	V_{DW}/(m/s)	Case	Δt_1/ms	V_{DW}/(m/s)
1.0	1.0	300	A1	-	2275	B1	0.6	2165
1.2	1.0	300	A2	0.3	2488	B2	0.39	2402
1.4	1.0	300	A3	0.26	2743	B3	0.26	2442
1.6	1.0	300	A4	0.48	2769	B4	-	2383
1.8	1.0	300	A5	0.72	2836	B5	-	-

4.3. Influence of Equivalent Ratio on RDRE Propulsion Performance

This section mainly studies the effect of equivalent ratio on RDRE propulsion performance. Specific impulse (I_{sp})is an important parameter for evaluating propulsive performance, so it is necessary to calculate I_{sp}. I_{sp} can be calculated by the following formula:

$$F = m_e v_e + (p_e - p_0)A_e \tag{12}$$

$$I_{sp} = \frac{F}{m_t g} \tag{13}$$

where F is the thrust of RDRE, m_t is the mass flow rate at the inlet of the plenum, m_e is the mass flow rate at the outlet of the RDR, v_e is the axial velocity at outlet of the RDRE, p_e is the static pressure at the outlet, p_0 is the environmental pressure at the outlet, A_e is the outlet area of RDRE, and g is the standard gravitational acceleration.

In order to eliminate the influence of the ignition stage, the data between 0.8 ms and 1.2 ms after the ignition were averaged in this paper. Figure 15 shows the average specific impulse (I_{spavg}) under different ER. When the number of injection holes is 60, the equivalent ratio increases from 1.0 to 1.8, and I_{spavg} increases from 192 s to 220 s by 14.6%. When the number of injection holes is 120, the equivalent ratio increases from 1.0 to 1.4 and from 192 s to 205 s, and the I_{spavg} of Case B4 under the unsteady detonation propagation mode is 237 s, but it has no reference value. The overall results show that when the equivalent ratio is between 1.0 and 1.8, the I_{sp} of RDRE increases with the increase of the equivalent ratio. We know that rocket engines can increase the specific impulse by increasing the gas temperature or decreasing the propellant molecular weight [50]. RDRE is consistent with conventional rocket engines, and the operating range of RDRE is different from ramjet RDE which is under lean fuel equivalent ratio. Figure 16 shows the average exit total temperature (T_{exit}) and molecular weight of the reactants (M_{molar}) of RDRE. The results demonstrate a decrease in T_{exit} and M_{molar} with an increase in the equivalent ratio.

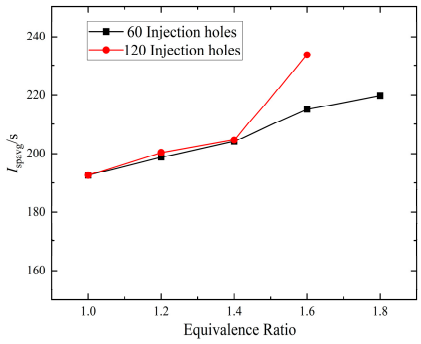

Figure 15. I_{spavg} under different equivalent ratios.

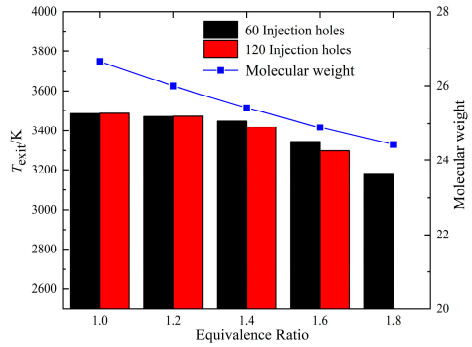

Figure 16. T_{exit} and M_{molar} under different equivalent ratios.

The curves of I_{sp} under different equivalent ratios are presented in Figure 17, exhibiting a significant oscillation during the initiation stage, which is caused by the blockage of part of the injection holes by irregular detonation waves that lead to the instability of inlet mass flow rate in the initiation stage. However, once the multi-wave stable propagation mode is reached, co-directional and regular RDWs have little effect on the blockage of injection holes and the specific impulse curve becomes stable. Under the condition of high equivalent ratio, case B4 experiences an unstable detonation mode leading to substantial oscillations in specific impulse. This instability arises due to variations in quantity, direction, and intensity of detonation waves and oblique shock waves within the RDRE flow field at different times during unstable detonation propagation mode, resulting in irregular and uneven gas expansion. Similarly, case A1 with a detonation-deflagration mixing mode also exhibits an unstable propagation mode with greater oscillation amplitude compared to other cases with 60 injection holes.

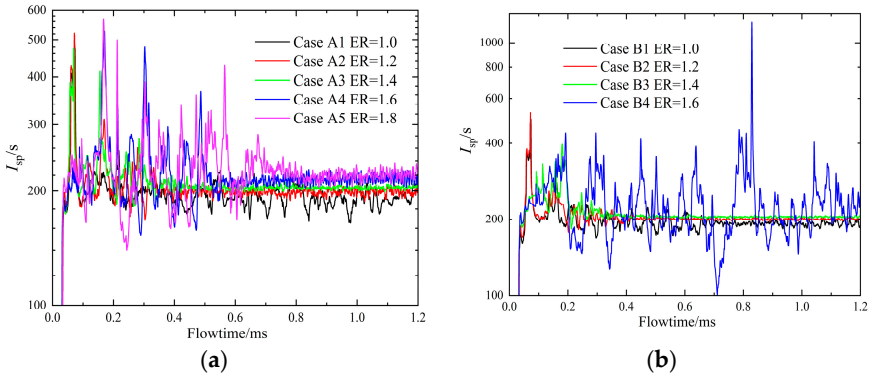

Figure 17. Specific impulse of different cases. (**a**) Specific impulse of cases with 60 injections holes. (**b**) Specific impulse of cases with 120 injections holes.

Figure 18 shows the standard deviation of thrust under different equivalent ratios between 0.8 ms and 1.2 ms after ignition. Standard deviation of thrust reflects the deviation degree between instantaneous thrust and average thrust. The thrust standard deviation of RDRE under unstable detonation propagation is greater than that under stable detonation propagation. In general, the thrust of RDRE is more stable in CMM, detonation waves are evenly distributed in RDRE and the spacing between oblique shock waves is uniform. The expansion of combustion products after oblique shock waves is more uniform and regular, thus generating more stable thrust. Combining the specific impulse and the stability of thrust, RDRE should be maintained in a state of co-directional multi-wave stable propagation to achieve more stable thrust within the range of the equivalent ratio where maximum specific impulse can be attained.

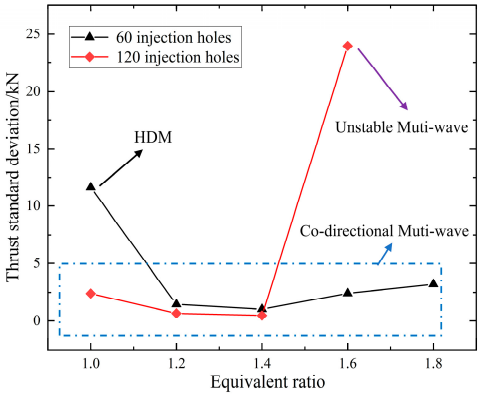

Figure 18. Standard deviation of thrust under different equivalent ratios.

5. Conclusions

In this study, two-dimensional numerical simulation of methane-oxygen RDRE was conducted. Two types of discrete injection holes were used to study the effects of different equivalent ratios (ER ranging from 1.0 to 1.8) on detonation characteristics and propulsion performance of RDRE. The conclusions are as follows:

(1) The numerical simulation results of this paper show that three distinct modes of detonation propagation are observed due to the influence of equivalent ratio and the number of injection holes. These modes include hybrid detonation mode, co-directional multi-wave detonation mode, and unstable detonation mode. The optimal propagation mode for RDRE is found to be the co-directional multi-wave detonation mode.

(2) The reactant activity has a significant influence on the flow field structure of RDRE. With the increase of equivalent ratio, the reactivity of the reactant decreases and the accumulated reaction heat in the strip deflagration regions decreases, which makes it difficult to induce more detonation waves. This leads to a decrease in the number of detonation waves and an increase in the height of both the reactant filling zone and the detonation waves.

(3) Owing to the presence of strip deflagration regions in the reactant filling zone, the accumulation of reaction heat under conditions approaching the stoichiometric ratio can readily induce the formation of new detonation waves, resulting in the unsteady propagation of detonation waves during the initiation stage. When the reactant activity is low, if the strip deflagration regions are large and concentrated, such as in cases with 60 injection holes, the accumulated heat can improve the activity of reactant and eventually lead to the formation of a stable co-directional multi-wave detonation mode; conversely, if the strip deflagration regions are small and dispersed, the accumulated reaction heat is insufficient to increase the reactant activity sufficiently to sustain a stable detonation propagation mode.

(4) Under fuel-rich conditions, the average specific impulse of RDRE increases with the increase of the equivalent ratio, which is consistent with the conventional rocket engines. Meanwhile, when RDRE operates in co-directional multi-wave detonation mode, it enhances the stability of both specific impulse and thrust, minimizing the oscillation amplitude of the specific impulse.

Author Contributions: Conceptualization, X.X.; methodology, X.X.; validation, X.X.; formal analysis, X.X.; investigation, X.X.; resources, Y.Z. and Q.H.; data curation, X.X.; writing—original draft preparation, X.X.; writing—review and editing, Q.H. and Y.Z.; supervision, Y.Z.; project administration, Y.Z. All authors have read and agreed to the published version of the manuscript.

Funding: This research received no external funding.

Data Availability Statement: The original contributions presented in this study are included in the article. Further inquiries can be directed to the corresponding author.

Conflicts of Interest: The authors declare no conflicts of interest.

References

1. Kailasanath, K. Review of propulsion applications of detonation waves. *AIAA J.* **2000**, *38*, 1698–1708. [CrossRef]
2. Zhao, X.; Wang, J.; Gao, L.; Wang, X.; Zhu, Y. Flame acceleration and onset of detonation in inhomogeneous mixture of hydrogen-air in an obstructed channel. *Aerosp. Sci. Technol.* **2022**, *130*, 107944. [CrossRef]
3. Zhao, X.; Wang, J.; Gao, L.; Pan, J.; Zhu, Y. Effect of hydrogen concentration distribution on flame acceleration and deflagration-to-detonation transition in staggered obstacle-laden channel. *Phys. Fluids* **2023**, *35*, 016124. [CrossRef]
4. Lu, F.K.; Braun, E.M. Rotating detonation wave propulsion: Experimental challenges, modeling, and engine concepts. *J. Propuls. Power* **2014**, *30*, 1125–1142. [CrossRef]

5. Zhou, R.; Wu, D.; Wang, J. Progress of continuously rotating detonation engines. *Chin. J. Aeronaut.* **2016**, *29*, 15–29. [CrossRef]
6. Zhou, S.; Ma, H.; Ma, Y.; Zhou, C.; Hu, N. Investigation on C_2H_4-Air combustion mode in a non-premixed rotating detonation combustor. *Propuls. Power Res.* **2022**, *11*, 85–96. [CrossRef]
7. Roy, G.; Frolov, S.; Borisov, A.; Netzer, D. Pulse detonation propulsion: Challenges, current status, and future perspective. *Prog. Energy Combust. Sci.* **2004**, *30*, 545–672. [CrossRef]
8. Anand, V.; George, A.S.; Driscoll, R.; Gutmark, E. Characterization of instabilities in a rotating detonation combustor. *Int. J. Hydrog. Energy* **2015**, *40*, 16649–16659. [CrossRef]
9. Anand, V.; George, A.S.; Gutmark, E. Amplitude modulated instability in reactants plenum of a rotating detonation combustor. *Int. J. Hydrog. Energy* **2017**, *42*, 12629–12644. [CrossRef]
10. Bykovskii, F.A.; Zhdan, S.A.; Vedernikov, E.F. Continuous spin detonations. *J. Propuls. Power* **2006**, *22*, 1204–1216. [CrossRef]
11. Fotia, M.L.; Schauer, F.; Kaemming, T.; Hoke, J. Experimental study of the performance of a rotating detonation engine with nozzle. *J. Propuls. Power* **2016**, *32*, 674–681. [CrossRef]
12. Russo, R.; King, P.; Schauer, F.; Thomas, L. Characterization of pressure rise across a continuous detonation engine. In Proceedings of the 47th AI-AA/ASME/SAE/ASEE Joint Propulsion Conference & Exhibit, San Diego, CA, USA, 31 July–3 August 2011; p. 6046. [CrossRef]
13. Anand, V.; George, A.S.; Driscoll, R.; Gutmark, E. Investigation of rotating detonation combustor operation with H_2-Air mixtures. *Int. J. Hydrog. Energy* **2016**, *41*, 1281–1292. [CrossRef]
14. Li, B.; Wu, Y.; Weng, C.; Zheng, Q.; Wei, W. Influence of equivalence ratio on the propagation characteristics of rotating detonation wave. *Exp. Therm. Fluid Sci.* **2018**, *93*, 366–378. [CrossRef]
15. Deng, L.; Ma, H.; Xu, C.; Liu, X.; Zhou, C. The feasibility of mode control in rotating detonation engine. *Appl. Therm. Eng.* **2018**, *129*, 1538–1550. [CrossRef]
16. Xie, Q.; Wen, H.; Li, W.; Ji, Z.; Wang, B.; Wolanski, P. Analysis of operating diagram for H2/Air rotating detonation combustors under lean fuel condition. *Energy* **2018**, *151*, 408–419. [CrossRef]
17. Wang, Y.; Wang, J. Effect of equivalence ratio on the velocity of rotating detonation. *Int. J. Hydrog. Energy* **2015**, *40*, 7949–7955. [CrossRef]
18. Zheng, H.; Meng, Q.; Zhao, N.; Li, Z.; Deng, F. Numerical investigation on H2/Air non-premixed rotating detonation engine under different equivalence ratios. *Int. J. Hydrog. Energy* **2020**, *45*, 2289–2307. [CrossRef]
19. Zhao, M.; Zhang, H. Origin and chaotic propagation of multiple rotating detonation waves in hydrogen/air mixtures. *Fuel* **2020**, *275*, 117986. [CrossRef]
20. Zhao, M.; Cleary, M.J.; Zhang, H. Combustion mode and wave multiplicity in rotating detonative combustion with separate reactant injection. *Combust. Flame* **2021**, *225*, 291–304. [CrossRef]
21. Lietz, C.; Ross, M.; Desai, Y.; Hargus, W.A.; Kailasanath, K.; Wilhite, J.; Driscoll, R.B.; George, A.C.S.; Anand, V.; Gutmark, E.J.; et al. Numerical investigation of operational performance in a methane-oxygen rotating detonation rocket engine. In Proceedings of the AIAA Scitech 2020 Forum, Orlando, FL, USA, 6–10 January 2020. [CrossRef]
22. Huang, Y.; Xia, H.; Chen, X.; Luan, Z.; You, Y. Shock dynamics and expansion characteristics of an aerospike nozzle and its interaction with the rotating detonation combustor. *Aerosp. Sci. Technol.* **2021**, *117*, 106969. [CrossRef]
23. Luan, Z.; Huang, Y.; Gao, S.; You, Y. Formation of multiple detonation waves in rotating detonation engines with inhomogeneous methane/oxygen mixtures under different equivalence ratios. *Combust. Flame* **2022**, *241*, 112091. [CrossRef]
24. Yao, S.; Liu, M.; Wang, J. Numerical investigation of spontaneous formation of multiple detonation wave fronts in rotating detonation engine. *Combust. Sci. Technol.* **2015**, *187*, 1867–1878. [CrossRef]
25. Wu, D.; Zhou, R.; Liu, M.; Wang, J. Numerical investigation of the stability of rotating detonation engines. *Combust. Sci. Technol.* **2014**, *186*, 1699–1715. [CrossRef]
26. Zhou, R.; Wang, J.-P. Numerical investigation of flow particle paths and thermodynamic performance of continuously rotating detonation engines. *Combust. Flame* **2012**, *159*, 3632–3645. [CrossRef]
27. Subramanian, S.; Meadows, J. Novel approach for computational modeling of a non-premixed rotating detonation engine. *J. Propuls. Power* **2020**, *36*, 617–631. [CrossRef]
28. Chen, H.; Si, C.; Wu, Y.; Hu, H.; Zhu, Y. Numerical investigation of the effect of equivalence ratio on the propagation characteristics and performance of rotating detonation engine. *Int. J. Hydrog. Energy* **2023**, *48*, 24074–24088. [CrossRef]
29. Menter, F.R. Two-equation eddy-viscosity turbulence models for engineering applications. *AIAA J.* **1994**, *32*, 1598–1605. [CrossRef]
30. Xu, R.; Dammati, S.S.; Shi, X.; Genter, E.S.; Jozefik, Z.; Harvazinski, M.E.; Lu, T.; Poludnenko, A.Y.; Sankaran, V.; Kerstein, A.R.; et al. Modeling of high-speed, methane-air, turbulent combustion, Part II: Reduced methane oxidation chemistry. *Combust. Flame* **2024**, *263*, 113380. [CrossRef]
31. Schau, K.A.; Oefelein, J.C. Numerical analysis of wave characteristics in a methane-oxygen rotating detonation engine. *AIAA J.* **2023**, *61*, 97–111. [CrossRef]

32. Smirnov, N.; Nikitin, V.; Stamov, L.; Mikhalchenko, E.; Tyurenkova, V. Three-dimensional modeling of rotating detonation in a ramjet engine. *Acta Astronaut.* **2019**, *163*, 168–176. [CrossRef]
33. Smirnov, N.; Nikitin, V.; Stamov, L.; Mikhalchenko, E.; Tyurenkova, V. Rotating detonation in a ramjet engine three-dimensional modeling. *Aerosp. Sci. Technol.* **2018**, *81*, 213–224. [CrossRef]
34. Liu, P.; Li, Q.; Huang, Z.; Zhang, H. Interpretation of wake instability at slip line in rotating detonation. *Int. J. Comput. Fluid Dyn.* **2018**, *32*, 379–394. [CrossRef]
35. Zhao, M.; Li, J.-M.; Teo, C.J.; Khoo, B.C.; Zhang, H. Effects of variable total pressures on instability and extinction of rotating detonation combustion. *Flow Turbul. Combust.* **2020**, *104*, 261–290. [CrossRef]
36. Schwer, D.; Kailasanath, K. Feedback into mixture plenums in rotating detonation engines. In Proceedings of the 50th AIAA Aerospace Sciences Meeting Including the New Horizons Forum and Aerospace Exposition, Nashville, TN, USA, 9–12 January 2012; p. 617. [CrossRef]
37. Liu, X.-Y.; Luan, M.-Y.; Chen, Y.-L.; Wang, J.-P. Propagation behavior of rotating detonation waves with premixed kerosene/air mixtures. *Fuel* **2021**, *294*, 120253. [CrossRef]
38. Wen, H.; Fan, W.; Xu, S.; Wang, B. Numerical study on droplet evaporation and propagation stability in normal-temperature two-phase rotating detonation system. *Aerosp. Sci. Technol.* **2023**, *138*, 108324. [CrossRef]
39. Li, Q.; Liu, P.; Zhang, H. Further investigations on the interface instability between fresh injections and burnt products in 2-D rotating detonation. *Comput. Fluids* **2018**, *170*, 261–272. [CrossRef]
40. Schwer, D.; Kailasanath, K. Numerical investigation of the physics of rotating-detonation-engines. *Proc. Combust. Inst.* **2011**, *33*, 2195–2202. [CrossRef]
41. Zhang, S.; Yao, S.; Luan, M.; Zhang, L.; Wang, J. Effects of injection conditions on the stability of rotating detonation waves. *Shock. Waves* **2018**, *28*, 1079–1087. [CrossRef]
42. NASA Glenn Research Center. *CEAgui-Win, Chemical Equilibrium with Applications GUI for Windows, Software Package, Version 28*; NASA Glenn Research Center: Cleveland, OH, USA, 2005.
43. Chacon, F.; Gamba, M. Study of parasitic combustion in an optically accessible continuous wave rotating detonation engine. In Proceedings of the AIAA Scitech 2019 Forum, San Diego, CA, USA, 7–11 January 2019. [CrossRef]
44. Burr, J.R.; Yu, K. Detonation wave propagation in cross-flow of discretely spaced reactant jets. In Proceedings of the 53rd AIAA/SAE/ASEE Joint Propulsion Conference, Atlanta, GA, USA, 10–12 July 2017; p. 4908. [CrossRef]
45. Hardalupas, Y.; Orain, M. Local measurements of the time-dependent heat release rate and equivalence ratio using chemiluminescent emission from a flame. *Combust. Flame* **2004**, *139*, 188–207. [CrossRef]
46. Röder, M.; Dreier, T.; Schulz, C. Simultaneous measurement of localized heat-release with OH/CH2O–LIF imaging and spatially integrated OH∗ chemiluminescence in turbulent swirl flames. *Proc. Combust. Inst.* **2013**, *34*, 3549–3556. [CrossRef]
47. Xia, Z.-J.; Luan, M.-Y.; Liu, X.-Y.; Wang, J.-P. Numerical simulation of wave mode transition in rotating detonation engine with OpenFOAM. *Int. J. Hydrog. Energy* **2020**, *45*, 19989–19995. [CrossRef]
48. Chen, H.; Si, C.; Hu, H.; Jin, Y.; Zhu, Y. Effects of the perturbation inlet on the evolution and oscillation characteristics of multiple rotating detonation waves. *Aerosp. Sci. Technol.* **2023**, *141*, 108586. [CrossRef]
49. Meng, H.; Weng, C.; Xiao, Q.; Zheng, Q.; Wu, Y.; Wang, F. Numerical analysis on evolution process of multiple rotating detonation waves with ethylene–oxygen–nitrogen mixture. *Proc. Inst. Mech. Eng. Part G J. Aerosp. Eng.* **2022**, *236*, 1304–1317. [CrossRef]
50. George, P.S.; Oscar, B. *Rocket Propulsion Elements*, 7th ed.; Science Press: Beijing, China, 2003; p. 38.